Biphasic function of GSK3β in gefitinib-resistant NSCLC with or without EGFR mutations

JUNZHE LI[1*], XIAYU WU[2*], XIANG-BO JI[3*], CHANGHAO HE[3], SHIJIE XU[3,4] and XIANHUA XU[2]

Departments of [1]Thoracic Surgery and [2]Pathology; [3]Medical Research Center, Affiliated Cancer Hospital of Hainan Medical University, Haikou, Hainan 570312, P.R. China; [4]Institute of Human Behavioral Medicine, Medical Research Center, Seoul National University, Seoul 03080, Republic of Korea

Abstract. Epidermal growth factor receptor-tyrosine kinase inhibitors (EGFR-TKIs), such as gefitinib, are effective in the treatment of non-small cell lung cancer (NSCLC) harboring EGFR mutations. However, the mechanism underlying acquired resistance to EGFR-TKIs remains largely unknown. Therefore, the present study generated gefitinib-resistant PC-9 (PC-9G) cells, which were revealed to be more resistant to gefitinib-induced reductions in proliferation, migration and invasion, and increases in apoptosis, and had no detectable EGFR mutations compared with the control PC-9 cell line. In addition, the present study performed genome-wide transcriptomic analysis of differentially expressed genes between PC-9 and PC-9G cell lines. Cell proliferation, colony formation, invasion, migration and flow cytometry analyses were also performed. The genome-wide transcriptomic analysis revealed that glycogen synthase kinase 3β (GSK3β) was downregulated in PC-9G cells compared with that in PC-9 cells. Furthermore, GSK3β overexpression increased the proliferation, migration and invasion of PC-9 and H1975 gefitinib-resistant cells. Conversely, overexpression of GSK3β suppressed the proliferation, migration and invasion of PC-9G cells. Furthermore, AKT inhibition reduced the proliferation, migration and invasion, and induced the apoptosis of PC-9, PC-9G and H1975 cells, the effects of which were reversed following AKT activation; notably, the tumor suppressor function of GSK3β

Correspondence to: Professor Shijie Xu, Medical Research Center, Affiliated Cancer Hospital of Hainan Medical University, 6 Changbin West Fourth Street, Haikou, Hainan 570312, P.R. China
E-mail: xushijie@nate.com

Professor Xianhua Xu, Department of Pathology, Affiliated Cancer Hospital of Hainan Medical University, 6 Changbin West Fourth Street, Haikou, Hainan 570312, P.R. China
E-mail: sunhwa@126.com

*Contributed equally

was inconsistent with the tumor promotor role of the AKT pathway in PC-9G cells without EGFR mutation. The present study may provide novel insights into the distinctive role of GSK3β in gefitinib-resistant NSCLC with or without EGFR mutations, suggesting that a more detailed investigation on GSK3β as a therapeutic target for gefitinib-resistant NSCLC may be warranted.

Introduction

Non-small cell lung cancer (NSCLC) accounts for ~80% of all lung cancer cases in worldwide (1). Epidermal growth factor receptor (EGFR)-targeted therapy is one of the main first-line treatments for NSCLC (2-4); however, almost all patients eventually develop acquired resistance to EGFR-tyrosine kinase inhibitors (TKIs) (5,6). The acquisition of EGFR-TKI resistance is associated with the EGFR-T790M gatekeeper mutation in patients with NSCLC treated with first-generation EGFR-TKIs, such as gefitinib or erlotinib (7-9). Notably, multiple mechanisms of acquired resistance to EGFR-TKIs have been reported, including MET receptor gene amplification (10), epithelial-mesenchymal transition (EMT) (11) and the pathological transformation of NSCLC to SCLC (12,13). However, other mechanisms underlying the acquired resistance to EGFR inhibitors remain to be discovered (12,14). To improve the effectiveness of EGFR-TKI treatment, a greater understanding of the unknown mechanisms underlying acquired resistance is urgently needed.

Glycogen synthase kinase 3β (GSK3β) is an isoform of the GSK3 family of kinases that promotes tumor development and progression in lung cancer (15,16). The tumor-promoting role of GSK3β is upregulated in NSCLC cells (17,18). Previous studies have shown that silencing GSK3β reduces the proliferation, migration and invasion, and increases the apoptosis of NSCLC cells (18,19). GSK3β also serves a pivotal role in the development of EGFR-resistant lung cancer. A previous study demonstrated that GSK3β inhibition suppresses the proliferation of cells with acquired resistance to osimertinib in EGFR-mutant NSCLC (20). However, little is currently known about the role of GSK3β in gefitinib-resistant NSCLC.

The present study aimed to investigate the role of GSK3β in gefitinib resistance in the PC-9 NSCLC cell line. Notably, GSK3β activity is often regulated by the PI3K/AKT or

Wnt signaling pathways in NSCLC (21). A previous study demonstrated that AKT activity is upregulated in cancer cells that are resistant to EGFR-TKIs (22). Furthermore, PI3K/AKT signaling is known to serve an important role in acquired resistance to EGFR-TKI in NSCLC (23-25). Therefore, the current study also examined the role of the PI3K/AKT pathway to explore whether it regulates GSK3β in EGFR-TKI-resistant cells.

Materials and methods

Cell culture and reagents. The human NSCLC cell lines PC-9 (exon 19 deletion) and H1975 (L858R/T790M) were kindly provided by The Cell Bank of Type Culture Collection of the Chinese Academy of Sciences. Gefitinib-resistant PC-9 cells were induced by gradually increasing drug concentrations. Briefly, $5x10^5$ cells in logarithmic phase were placed in RPMI-1640 medium (cat. no. C11875500BT; Gibco; Thermo Fisher Scientific, Inc.) supplemented with 10% fetal bovine serum (FBS; cat. no. ST30-3302; PAN-Biotech GmbH) and 1% penicillin-streptomycin (cat. no. 15140-122; Gibco; Thermo Fisher Scientific, Inc.) at 37°C with 5% CO_2. After 24 h of adherence, 100 nmol/l gefitinib (cat. no. HY-50895; MedChemExpress) was used as the initial concentration to treat cells, and the medium containing gefitinib was changed daily. After 3-4 weeks, the cells gradually showed tolerance and stable growth, were cultured in normal medium for 3-5 days, then passaged, and the concentration of gefitinib was doubled again until the concentration had been doubled five times. The final drug concentration was 3.2 μmol/l, which was maintained for 1 month, after which, the medium was replaced with drug-free medium for 1 month. The whole process took 7 months to complete, and the established resistant cell line was named PC-9G. The cells were cultured in RPMI-1640 medium (cat. no. C11875500BT; Gibco; Thermo Fisher Scientific, Inc.) supplemented with 10% fetal bovine serum (FBS; cat. no. ST30-3302; PAN-Biotech GmbH) and 1% penicillin-streptomycin (cat. no. 15140-122; Gibco; Thermo Fisher Scientific, Inc.). All cells were maintained in a 37°C incubator with 5% CO_2. SC79 (AKT activator, 5 nmol/l; cat. no. HY-18749; MedChemExpress) and MK2206 (AKT antagonist, 5 nmol/l; cat. no. HY-10358; MedChemExpress) were dissolved in 0.5% DMSO. The images of cell fluorescence were obtained using a fluorescence microscope (Olympus IX73; Olympus Corporation). Cell morphology was assessed by light microscopy (Olympus BX53; Olympus Corporation).

Cell proliferation assay. The human NSCLC cell lines PC-9, PC-9G and H1975 were seeded into 96-well plates ($1.5x10^3$ cells/well) and were treated with gefitinib (0, 1, 5, 10, 50, 100, 1,000, 5,000, 10,000 or 50,000 nmol/l). Following incubation for 72 h at 37°C with 5% CO_2, a Cell Counting Kit-8 (CCK8) kit (Vazyme Biotech Co., Ltd.) was used to determine cell viability and proliferation. Fresh medium was used to replace the old medium, and 10 μl CCK-8 reagent was added to each well. Cell viability was measured at a wavelength of 450 nm, and cell proliferation was calculated as optical density (OD) value of the experimental well/OD value of control well (day 1). The results were obtained using five replicates per experiment from three separate experiments.

Colony formation assay. The human NSCLC cell lines PC-9 and PC-9G were seeded into six-well plates ($1x10^4$ cells/well) and were treated with gefitinib (300 nmol/l) or 0.3% DMSO. The drugs were changed every 3 days and cells were cultured at 37°C with 5% CO_2. After 10 days, cell colonies were fixed with 4% paraformaldehyde (MilliporeSigma) at room temperature for 30 min, and then stained with 0.05% violet crystal (MilliporeSigma) at room temperature for 30 min. After washing three times with PBS, the number of colonies >1 mm in size was counted manually in each group.

Migration assays. Following treatment with MK2206 (AKT inhibitor, 5 nmol/l) or SC79 (AKT activator, 5 nmol/l) at 37°C for 24 h, PC-9 and PC-9G ($6x10^4$/well), and H1975 ($3x10^4$/well) cells were seeded in 24-well migration chambers (pore size, 8-μm; Corning, Inc.) containing RPMI-1640 without FBS, and 400 μl RPMI-1640 supplemented with 10% FBS was added to the lower chamber to stimulate cell migration. After incubation at 37°C for 18-24 h, non-migratory cells were removed from the upper chamber with a cotton swab, and the cells that had migrated to the lower chamber were fixed with 20% methanol at room temperature for 30 min, and then stained with 0.1% crystal violet at room temperature for 30 min. Migratory cells were counted using a light microscope and analyzed based on four randomly selected fields.

Invasion assays. Following treatment with MK2206 (5 nmol/l) or SC79 (5 nmol/l) at 37°C for 24 h, PC-9 and PC-9G ($1.5x10^5$/well), and H1975 ($1x10^5$/well) cells were seeded in 24-well Transwell units (pore size, 8-μm; Corning, Inc.) containing RPMI-1640 without FBS, and 400 μl RPMI-1640 supplemented with 10% FBS was added to the lower chamber to stimulate cell invasion. After precoating the chambers with 3 mg/ml Matrigel (Corning, Inc.) at 37°C for 30 min, cells were added to 24-well Transwell chambers. After incubation at 37°C for 18-24 h, non-invasive cells were removed from the upper chamber with a cotton swab, and the cells that had invaded the lower chamber were fixed with 20% methanol at room temperature for 30 min, and then stained with 0.1% crystal violet at room temperature for 30 min. Invasive cells were counted using a light microscope and analyzed based on four randomly selected fields.

Apoptosis assay. PC-9, PC-9G and H1975 cells were seeded into 60-mm dishes ($5x10^5$ cells) and treated with gefitinib (300 nM) or DMSO (negative control). After incubation at 37°C for 48 h, the cells were harvested and stained with annexin V-fluorescein isothiocyanate (FITC) and propidium iodide (PI) (Vazyme Biotech Col., Ltd.) at room temperature for 15 min in the dark. BD FACSCanto (BD Biosciences) was used to measure the fluorescence intensity in the FITC (FL1, 533 nm) and PI (FL2, 585 nm) channels. Early apoptotic cells (annexin V-positive only) and late apoptotic cells (annexin V- and PI-positive) were quantified and analyzed using FlowJo 10.0.7 software (FlowJo LLC).

RNA-sequencing (RNA-seq). To obtain the differential gene expression profile between PC-9 and PC-9G cells, total RNA was extracted from PC-9 and PC-9G cells (10^5-10^6 cells) using TRIzol® reagent (cat. no. 15596026CN; Invitrogen; Thermo

Fisher Scientific, Inc.) according to the manufacturer's instructions. The quantity and quality of RNA were evaluated using an Agilent 2100 Bioanalyzer (Agilent Technologies, Inc.). Samples (1 μg) with an RNA integrity number score of >7 and RNA concentration of >1,000 ng were selected for library preparation. After quantification of nucleic acid extraction, the NEB Next rRNA Depletion Kit (cat. no. E6310S; New England BioLabs, Inc.) was used to remove rRNA. The rRNA-depleted product was subjected to reverse transcription (RT) and double-stranded cDNA synthesis using M-MLV Reverse Transcriptase, RNase H Minus, Point Mutant (cat. no. M3683; Promega Corporation) and NEBNext Ultra II Non-Directional RNA Second Stand Synthesis Module (cat. no. E6111S; New England BioLabs, Inc). The double-stranded cDNA was then fragmented using Covaris LE220-plus shearing instrument (Covaris, LLC). Library construction was performed using the KAPA Hyper Prep kit (cat. no. KK8504; Kapa Biosystems; Roche Diagnostics), and the library was quantified using Qubit® dsDNA HS Assay Kit (Thermo Fisher Scientific, Inc.). The size distribution of library fragments was analyzed using LabChip GX Touch HT DNA High Sensitivity Assay Kit (PerkinElmer, Inc.). The whole transcriptome sequencing library was denatured and diluted to a concentration of 200-250 pM and sequenced on Illumina NovaSeq 6000 sequencing platform (cat. no. 20012850; Illumina, Inc.). The sequencing strategy was paired-end 150 bp, and the sequencing chip used was NovaSeq 6000 S1 Reagent Kit (300 cycles) (cat. no. 20012863; Illumina, Inc.). The required data output was 10 M reads. The raw data obtained from sequencing were evaluated with FastQC (0.11.5; https://github.com/pnnl/fqc). After removing adapters and low-quality sequences using AdapterRemoval (2.2.2; https://github.com/MikkelSchubert/adapterremoval), clean reads were obtained. Subsequently, STAR (2.5.3a;https://github.com/alexdobin/STAR) was used to align the clean reads to the hg19 whole transcriptome sequence. RSEM (1.3.0; http://deweylab.biostat.wisc.edu/rsem) was used for gene expression quantification. Differential expression analysis was performed using edgeR (3.28.1;http://bioconductor.org/packages/3.2/bioc/html/edgeR.html) with default parameters, and differentially expressed genes (DEGs) were identified as|log2(fold change)|>1 and FDR<0.05. Finally, the pheatmap (V 1.0.12; https://cran.r-project.org/web/packages/pheatmap/index.html)was used to create a heatmap. KEGG functional enrichment analysis was performed using org.hs.eg. DB (26). To process the functional enrichment analysis, when the corrected P-value, that is q-value, was ≤0.05, the KEGG function was considered to be significantly enriched. ggplot2 (3.3.5; https://github.com/JLSteenwyk/ggpubfigs.) was used for plotting the enriched signaling pathway.

Lentiviral packaging and stable cell line establishment. The gene sequences of GSK3β were synthesized and cloned into pCDH-GFP-puro (pCDH) lentiviral vectors (Generay Biotech Co., Ltd.). To produce the lentivirus, 1 μg pMD2.G and 3 μg psPAX2 were cotransfected with PCDH-GSK3β (4 μg) or the vehicle plasmid (PCDH, 4 μg) into 293T cells using the Nano293T Transfection Reagent (cat. no. C500T-1; NCM Biotech) at 37°C for 12 h. Lentiviral particles (PCDH and PCDH-GSK3β) were harvested at three timepoints (24, 48 and 72 h) after transfection and all of the individual harvests were pooled for infection. The multiplicity of infection for PC-9, PC-9G and H1975 cells was 20, 40 and 10, respectively. After 24 h infection with the cells, the medium was changed. PC-9, PC-9G and H1975 cells were screened with 6 μg/ml puromycin (Beijing Solarbio Science & Technology Co., Ltd.) for 2-3 times to obtain a stably transduced cell line. After puromycin screening for 3 weeks, stable cell lines PC-9/PCDH, PC-9/GSK3β, PC-9G/PCDH, PC-9G/GSK3β, H1975/PCDH and H1975/GSK3β were established and used in subsequent experiments.

RT-quantitative PCR (RT-qPCR). Total RNA was isolated from PC-9, PC-9G and H1975 cells, as well as cells stably overexpressing GSK3β (PC-9/GSK3β, PC-9G/GSK3β, H1975/GSK3β) and those infected with an empty vector (PC-9/PCDH, PC-9G/PCDH, and H1975/PCDH) using the FastPure Cell RNA Isolation Kit V2 (cat. no. RC112; Vazyme Biotech Co., Ltd.). RNA was reverse transcribed into cDNA using a RT kit (cat. no. R323-01; Vazyme Biotech Co., Ltd.) according to the manufacturer's instructions. Subsequently cDNA was subjected to qPCR using SYBR Green Mix (Vazyme Biotech Co., Ltd.). The qPCR protocol was as follows: 95°C for 5 min; followed by 40 cycles of denaturation at 95°C for 10 sec, and annealing and extension at 60°C for 30 sec; with a final fluorescence measurement at 60°C. The relative expression levels of the target genes were determined using the comparative cycle threshold method ($2^{-\Delta\Delta Cq}$) (27). The primer sequences were as follows: GSK3β forward, 5'-AGAGACAAG GACGGCAGCAAG-3' and reverse, 5'-GATGGCGACCAG TTCTCCTG-3'; GAPDH forward, 5'-GTCTCCTCTGACTTC AACAGCG-3' and reverse, 5'-ACCACCCTGTTGCTGTAG CCAA-3'.

Nuclear/cytoplasmic protein separation and extraction. Nuclear and cytosolic proteins were extracted using a nucleocytoplasmic separation and extraction kit (Thermo Fisher Scientific, Inc.) according to the manufacturer's protocols. The supernatants were collected and then analyzed by western blotting.

Protein extraction and western blot analysis. Following 24 h of treatment with the AKT activator or inhibitor at 37°C, PC-9, PC-9G and H1975 cells were harvested, and total protein was extracted using radioimmunoprecipitation assay lysis buffer (Beyotime Institute of Biotechnology) supplemented with protease inhibitors for 15 min. Proteins were then centrifuged at 16,000 x g for 15 min at 4°C. These steps were all performed on ice. The supernatants were collected and protein concentration was determined via bicinchoninic acid assay (Thermo Scientific Fisher Scientific, Inc.). Subsequently, the proteins were subjected to western blot analysis according to the manufacturer's instructions (CWBio), after which an ECL Detection System (Thermo Fisher Scientific, Inc.) was used for signal detection. Protein bands were semi-quantified using ImageJ analysis software (version 1.8.0; National Institutes of Health). Equal amounts of heat-denatured protein (30 μg/lane) were separated by SDS-PAGE on 10% gels and transferred onto nitrocellulose membranes, which were blocked with blocking buffer containing 5% non-fat milk in 1X TBS-0.1% Tween-20 for 2 h at room temperature and incubated with primary

antibodies at 4˚C overnight, followed by incubation with an appropriate secondary antibody at 37˚C for 2 h. The following primary antibodies (1:1,000 dilution; all from Cell Signaling Technology, Inc.) were used: c-Myc (cat. no. 5605), E-cadherin (cat. no. 3195), vimentin (cat. no. 5741), GAPDH (cat. no. 5174), β-catenin (cat. no. 8480), Lamin A (cat. no. 86846), GSK3β (cat. no. 12456), phosphorylated (p)GSK3β (cat. no. 9322), AKT (cat. no. 4691), pAKT (cat. no. 4060), MET (cat. no. 8198), pMET (cat. no. 3077), and β-actin (cat. no. 8457). The secondary antibodies used were horseradish peroxidase-conjugated goat anti-rabbit IgG secondary antibody (cat. no. L3012; 1:5,000 dilution; SAB Biotherapeutics, Inc.) and anti-mouse IgG secondary antibody (cat. no. L3032; 1:5,000 dilution; SAB Biotherapeutics, Inc.).

Immunohistochemistry. Immunohistochemistry was performed to determine E-cadherin and vimentin expression levels in PC-9 and PC-9G cells without any treatment. PC-9 and PC-9G cells were fixed with Bouin's solution containing 5% acetic acid, 9% formaldehyde and 0.9% picric acid (Millipore Sigma) at room temperature for 24 h, washed with 70% ethanol and embedded in paraffin. The sections (5 μm) were then deparaffinized in xylene, hydrated in a graded series of ethanol and placed in a solution of sodium citrate (pH 6.0) under high-pressure heat-mediated antigen retrieval for 3 min. Subsequently, the slides were probed with E-cadherin (cat. no. 3195, 1:400 dilution; Cell Signaling Technology, Inc.) and vimentin (cat. no. 5741, 1:100 dilution; Cell Signaling Technology, Inc.) antibodies overnight at room temperature. After incubation with HRP-conjugated secondary antibody (cat. no. #K8000; 1:1,000; Agilent Technologies, Inc.) at room temperature for 30 min, the signal was developed using the DAB Histochemistry Kit (Invitrogen; Thermo Fisher Scientific, Inc.). The images were visualized using a light microscope.

Statistical analysis. Data are presented as the mean ± SD of at least three independent experiments. Statistical differences were analyzed by an independent samples t-test. All data were analyzed using GraphPad Prism version 8 software (Dotmatics). $P<0.05$ was considered to indicate a statistically significant difference.

Results

Successful generation of PC-9G cells in vitro. PC-9G cells were successfully constructed *in vitro* by increasing the drug concentration for 10 months. The results of the CCK8 assay showed that the half maximal inhibitory concentration (IC_{50}) values of PC-9 and PC-9G cells were 637.3±0.21 nmol/l and 3.37±0.13 μmol/l, respectively, and the resistant index was 52.91 (Fig. 1A). Notably, neither EGFR mutations or MET exon 14 skipping mutation were detected in PC-9G cells (Fig. S1). To further elucidate the effect of gefitinib on the colony formation of PC-9 and PC-9G cells, 300 nmol/l gefitinib was used to treat the cells. The results showed that the colony formation of PC-9 cells was significantly decreased following gefitinib treatment; however, the clonogenic ability of PC-9G cells was not significantly affected by gefitinib (Fig. 1B). The proliferation of the cells was also assessed using the CCK8 kit and was

significantly higher in PC-9G cells than in PC-9 cells without gefitinib treatment (Fig. 1C). PC-9G cells were well defined and showed a mesenchymal phenotype, including a spindle appearance and loss of intercellular connections, and some cells had prominent pseudopodia compared with PC-9 cells (Fig. 1D). Furthermore, the apoptotic rate of PC-9G cells was lower than that of PC-9 cells. It was further verified that 300 nmol/l gefitinib significantly increased the apoptosis of PC-9 cells, but did not significantly affect the apoptosis of PC-9G cells (Fig. 1E). Migration and invasion assays showed that PC-9G cells had significantly enhanced migration (Fig. 1F) and invasion (Fig. 1G) compared with PC-9 cells without gefitinib treatment. These results indicated that PC-9G cells were successfully established *in vitro*.

RNA-seq of PC-9 and PC-9G cells. To further investigate the molecular mechanism underlying PC-9 resistance to gefitinib, RNA-seq was performed to compare PC-9 and PC-9G cells. KEGG pathway enrichment analysis showed that DEGs between PC-9 and PC-9G cells were enriched in 'PI3K-AKT signaling pathway', 'herpes simplex virus 1 infection' and 'MAPK signaling pathway' (Fig. 2A). In addition, heatmap clustering analysis of PI3K-AKT signaling pathway-related genes was conducted and the gene that was the most downregulated in PC-9G cells compared with in PC-9 cells, GSK3β, was selected for further analysis (Fig. 2B). The phosphorylation and expression of GSK3β and AKT were assessed in PC-9 and PC-9G cells following treatment with 300 nmol/l gefitinib (Figs. 2C and S2). The protein expression levels of pGSK3β and total GSK3β were lower in PC-9G cells than those in PC-9 cells. Following gefitinib treatment, the expression levels of pGSK3β in PC-9 cells were increased, whereas the phosphorylation of GSK3β in PC-9G cells was decreased. Furthermore, AKT phosphorylation in PC-9G cells was markedly decreased compared with that in PC-9 cells. The expression of c-Myc was higher in PC-9G cells than that in PC-9 cells, but was decreased by treatment with gefitinib in both PC-9 and PC-9G cells; notably, c-Myc is known to positively regulate cell proliferation (28). Furthermore, the expression levels of E-cadherin were lower in PC-9G cells than those in PC-9 cells, whereas the expression levels of vimentin were higher in PC-9G cells than those in PC-9 cells; these proteins are closely related to metastasis (29). These results indicated that the EMT of PC-9G cells was increased, which was consistent with the results of the migration and invasion assays (Fig. 2C). Immunohistochemistry results also confirmed that E-cadherin expression was strongly membrane-positive in PC-9 cells and negative in PC-9G cells. By contrast, vimentin expression was negative in PC-9 cells and strongly positive in PC-9G cells (Fig. 2D). These results indicated that GSK3β was downregulated in gefitinib-resistant cells, which is related to cell proliferation and metastasis.

Effects of GSK3β overexpression on the proliferation, apoptosis, migration and invasion of PC-9, PC-9G and H1975 cells. To determine the function of GSK3β in PC-9G cells, GSK3β was overexpressed in PC-9, PC-9G and H1975 cells using lentiviral vectors. Cell fluorescence analysis showed that the overexpression was successful in PC-9, PC-9G and H1975 cells (Fig. 3A). The protein and mRNA expression levels of
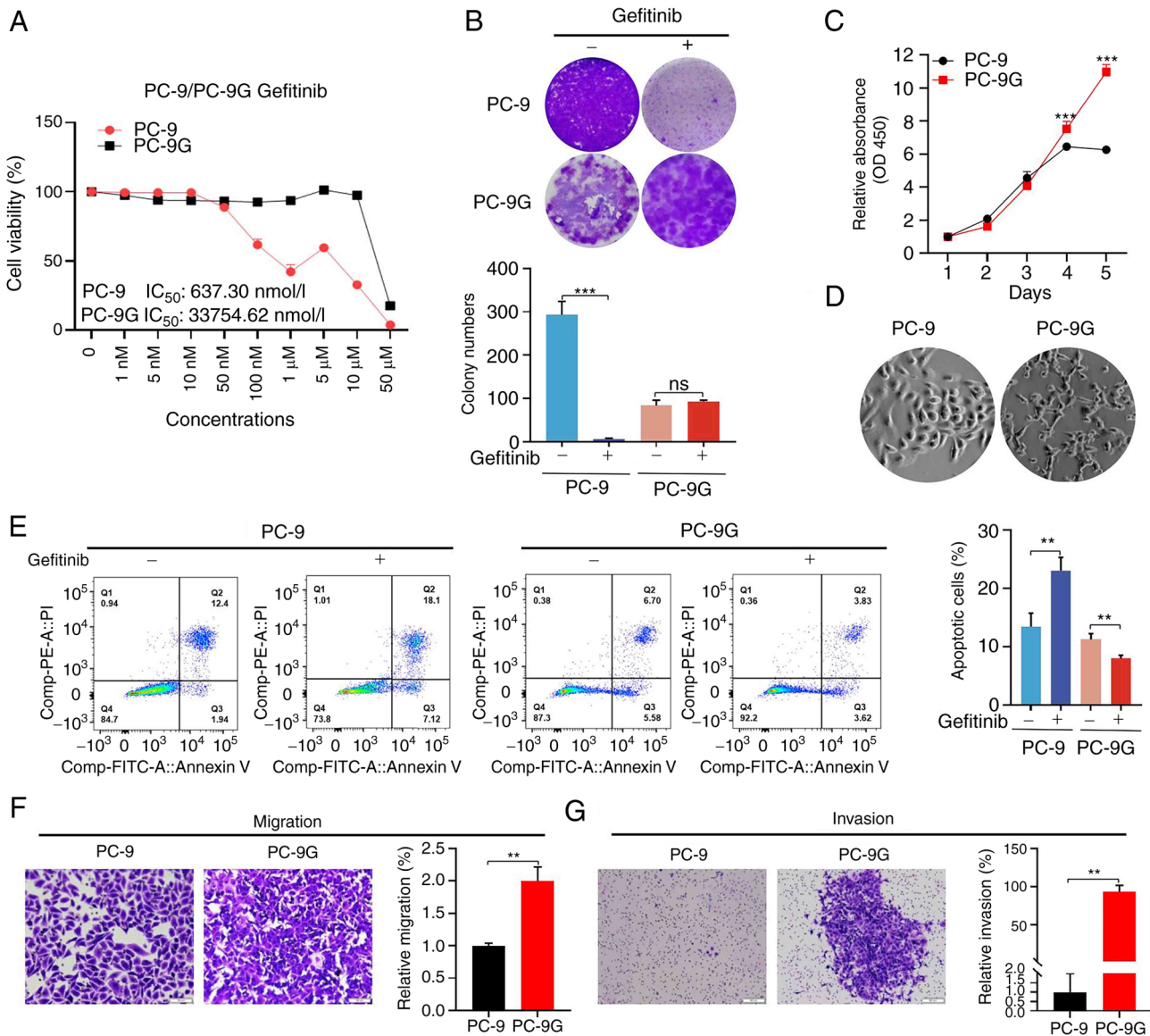
Figure 1. PC-9G cells were generated *in vitro*. (A) Results of Cell Counting Kit-8 assay showed that the IC$_{50}$ of PC-9 and PC-9G cells was 637.3±0.21 nmol/l and 3.37±0.13 μmol/l, respectively, and the resistant index was 52.91. (B) Colony formation assay of PC-9 and PC-9G cells. The results showed that gefitinib inhibited the colony formation of PC-9 cells. (C) Proliferation of PC-9G cells was significantly higher than that of PC-9 cells. (D) Morphology of PC-9 and PC-9G cells under a microscope (magnification, x20). (E) Gefitinib increased the apoptosis of PC-9 cells but decreased the apoptosis of PC-9G cells. (F) Migration and (G) invasion of PC-9G cells was significantly higher than that of PC-9 cells (magnification, x20). Data are presented as the mean ± SD of three independent experiments. **$P<0.01$, ***$P<0.001$ vs. PC-9 or as indicated. FITC, fluorescein isothiocyanate; IC$_{50}$, half maximal inhibitory concentration; PC-9G, gefitinib-resistant PC-9; PI, propidium iodide.

GSK3β were markedly increased in PC-9, PC-9G and H1975 cells post-infection (Fig. 3B and C), indicating that infection with lentiviral vectors stably expressing GSK3β was successful compared with the empty vector control. In addition, the expression levels of c-Myc were reduced by GSK3β overexpression in PC-9, PC-9G and H1975 cells compared with those in the empty vector control (Figs. 3C and S3). However, the expression of vimentin was not induced by GSK3β overexpression in PC-9, PC-9G and H1975 cells compared with that in the empty vector control. In addition, GSK3β overexpression did not induce the expression of E-cadherin in PC-9 and PC-9G cells, but its overexpression inhibited E-cadherin expression in H1975 cells compared with that in the empty vector control. Moreover, cytoplasmic and nuclear β-catenin expression was reduced by overexpression of GSK3β in PC-9 and H1975

cells, but not in PC-9G cells, compared with that in the control group (Fig. 3C). Furthermore, overexpression of GSK3β increased the cell proliferation, invasion and migration of both PC-9 and H1975 cells compared with that in the empty vector control group, whereas it suppressed the proliferation, invasion and migration of PC-9G cells (Fig. 3D-F). Taken together, these results suggested that GSK3β overexpression exhibited opposite effects between resistant and parental cell lines.

Effects of an AKT inhibitor on the proliferation, apoptosis, migration and invasion of PC-9, PC-9G and H1975 cells. To further determine whether GSK3β overexpression suppressed the proliferation, migration and invasion of PC-9G cells via the PI3K/AKT signaling pathway, PC-9, PC-9G and H1975 cells were treated with 5 nM MK2206 (AKT antagonist). Treatment
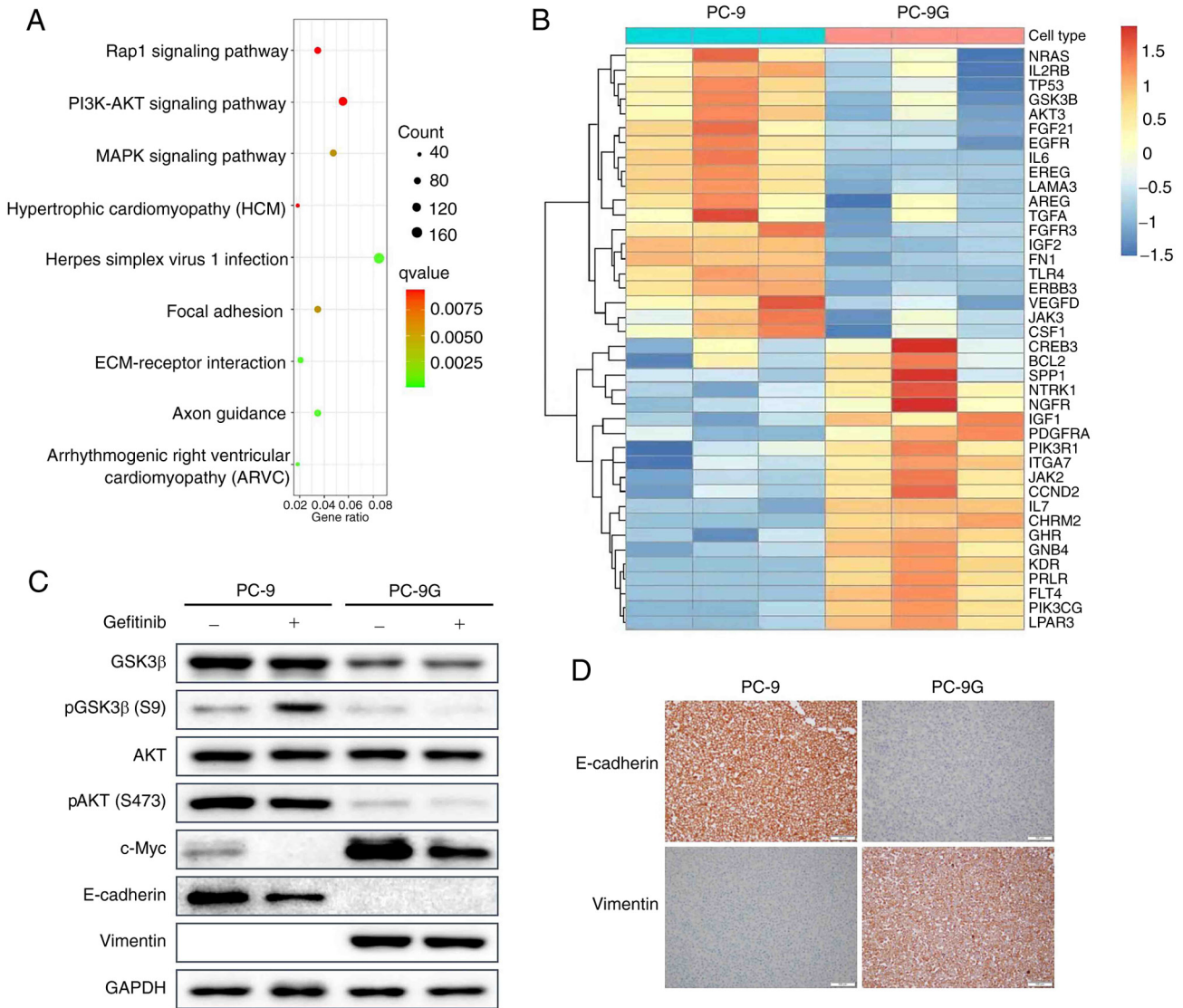
Figure 2. GSK3β is involved in gefitinib resistance in PC-9G cells. (A) Genes related to the PI3K-AKT signaling pathway were differentially expressed between PC-9 and PC-9G cells. (B) Heatmap clustering analysis of differentially expressed genes between PC-9 and PC-9G cells. (C) Protein expression levels of GSK3β, pGSK3β (Ser9), AKT, pAKT (Ser473), c-Myc, E-cadherin and vimentin were detected via western blot analysis in PC-9 and PC-9G cells treated with DMSO or 300 nmol/l gefitinib. (D) Immunohistochemical analysis showed that the expression of E-cadherin in PC-9 cells was higher than that in PC-9G cells, whereas the expression of vimentin in PC-9 cells was lower than that in PC-9G cells (magnification, x20). GSK3β, glycogen synthase kinase 3β; p, phosphorylated; PC-9G, gefitinib-resistant PC-9.

with MK2206 significantly increased the phosphorylation of GSK3β in PC-9, PC-9G and H1975 cells compared with that in the control group (Figs. 4A and S4). In addition, the expression of c-Myc was decreased by MK2206 treatment in PC-9, PC-9G and H1975 cells. However, MK2206 treatment did not alter the expression levels of E-cadherin or vimentin in PC-9, PC-9G and H1975 cells compared with those in the control group. Moreover, MK2206 treatment increased the apoptotic rate of PC-9, PC-9G and H1975 cells (Fig. 4B and D). Additionally, MK2206 treatment inhibited the proliferation of H1975 cells, and it reduced the proliferation of PC-9 cells on day 5 of treatment (Fig. 4C). Furthermore, treatment with 2206 reduced the migration and invasion of PC-9, PC-9G and H1975 cells compared with the control group (Fig. 4E and F). These findings indicated that AKT inhibition could increase the apoptosis, and reduce the migration and invasion of PC-9, PC-9G and H1975 cells.

Effects of an AKT activator on the proliferation, apoptosis, migration and invasion of PC-9, PC-9G and H1975 cells. To further examine whether AKT activation could affect the proliferation, migration and invasion of gefitinib-resistant cells, PC-9, PC-9G and H1975 cells were treated with 5 nM SC79 (AKT activator). Phosphorylation of AKT was increased by treatment with SC79 in PC-9, PC-9G and H1975 cells (Figs. 5A and S5). However, GSK3β phosphorylation was not altered by treatment with SC79 in PC-9, PC-9G and H1975 cells compared with that in the control group. The expression of c-Myc in PC-9 and H1975 cells was significantly increased following SC79 treatment, whereas that in PC-9G cells was significantly decreased. In addition, the expression levels of E-cadherin and vimentin were not altered by SC79 treatment in PC-9, PC-9G and H1975 cells when compared with those in the control group. Moreover, SC79 treatment reduced the apoptotic rate in PC-9 cells, but not in PC-9G and H1975 cells,
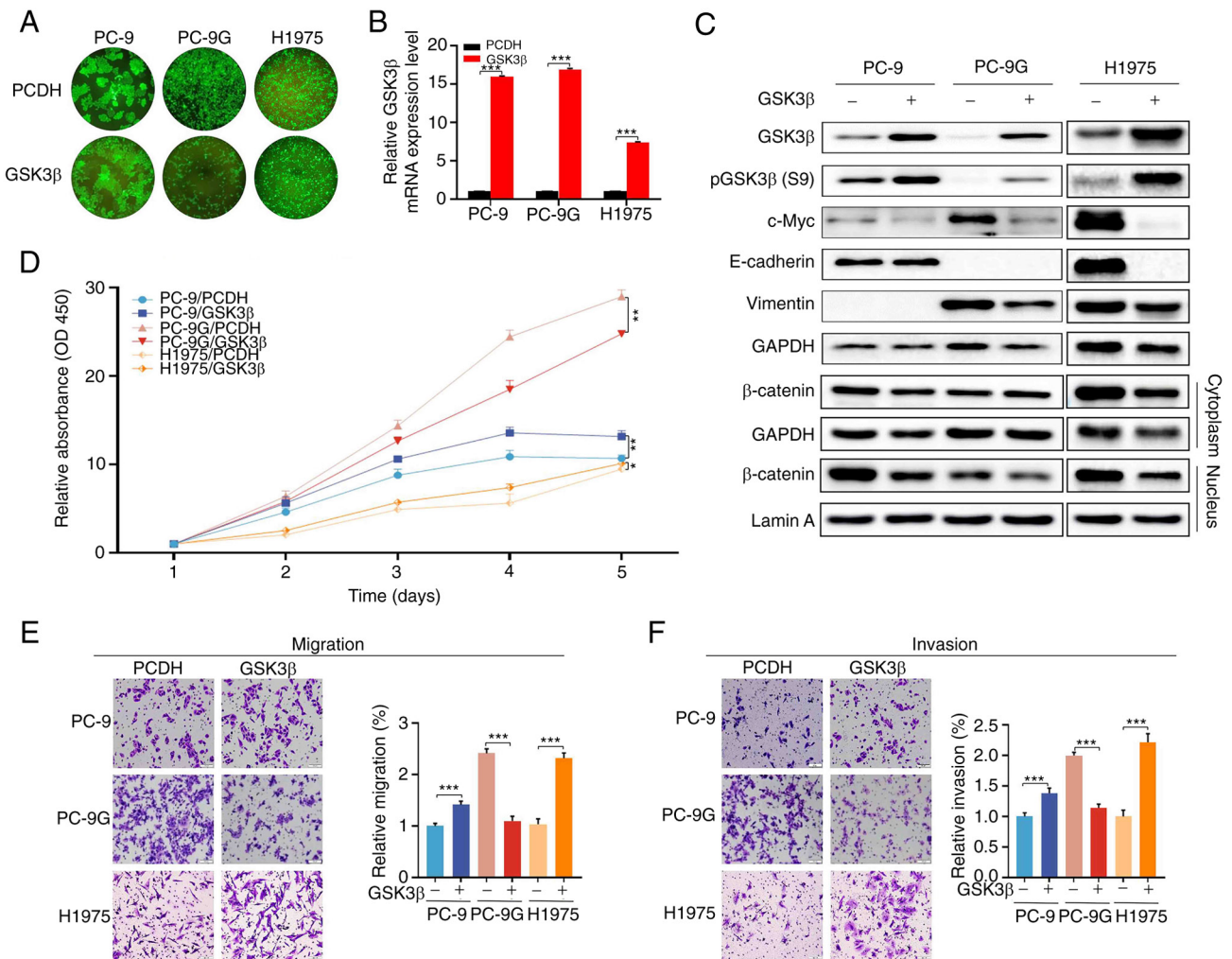
Figure 3. Effects of GSK3β overexpression on the proliferation, migration and invasion of PC-9, PC-9G and H1975 cells. (A) Fluorescence microscopy showed that stable GSK3β overexpression was successfully achieved in PC-9, PC-9G and H1975 cells (magnification, x10). (B) mRNA expression levels of GSK3β were upregulated in PC-9, PC-9G and H1975 cell lines with stable GSK3β overexpression. (C) Protein expression levels of GSK3β, pGSK3β (Ser9), c-Myc, E-cadherin, vimentin and β-catenin was determined via western blot analysis in PC-9, PC-9G and H1975 cells following overexpression of GSK3β. (D) GSK3β overexpression enhanced the proliferation of PC-9 and H1975 cells, but not that of PC-9G cells. GSK3β overexpression reduced the (E) migration and (F) invasion of PC-9G cells, but enhanced the migration and invasion of PC-9 and H1975 cells (magnification, x20). Data are presented as the mean ± SD of three independent experiments. $^{*}P<0.05$, $^{**}P<0.01$, $^{***}P<0.001$. GSK3β, glycogen synthase kinase 3β; p, phosphorylated; PC-9G, gefitinib-resistant PC-9.

compared with that in the control group (Fig. 5B and D). The proliferation of H1975 cells increased from day 3 to 5 after SC79 treatment, whereas the proliferation of PC-9 cells, but not PC-9G cells, increased on day 5 after SC79 treatment (Fig. 5D). Furthermore, SC79 treatment increased the migration and invasion of PC-9, PC-9G and H1975 cells compared with those in the control group (Fig. 5E and F). Collectively, these results suggested that AKT activation attenuated the apoptosis of PC-9 cells, and enhanced the migration and invasion of PC-9G cells, and GSK3β was not associated with the AKT pathway in PC-9G cells.

Discussion

In previous studies, PC-9 cells with acquired resistance to gefitinib exhibited an EGFR mutation (deletion of exon 19) or generated a second EGFR-T790M mutation (30,31). However, in the present study, the PC-9G gefitinib-resistant cell line did not exhibit EGFR mutations, thus indicating that the

mechanisms of acquired resistance to EGFR-TKIs are not always associated with EGFR mutations and suggesting that different molecular mechanisms may be involved in the resistance to gefitinib. Analysis of differentially expressed genes between PC-9 and PC-9G cell lines revealed that GSK3β was downregulated in PC-9G cells compared with that in PC-9 cells. In addition, overexpression of GSK3β decreased c-Myc expression in PC-9G cells, which was associated with cell proliferation, and the expression of the EMT-associated proteins vimentin was reduced by overexpression of GSK3β. Furthermore, overexpression of GSK3β suppressed the proliferation, migration and invasion of PC-9G cell lines, whereas it promoted the proliferation, migration and invasion of the PC-9 and H1975 cell lines. In general, GSK3β is upregulated as a tumor promoter in NSCLC cells (17,18). A previous study demonstrated that silencing GSK3β can significantly decrease the proliferation of resistant cells harboring the EGFR T790M and L858R mutations (20). In the present study, GSK3β was identified as a tumor suppressor in PC-9G cells
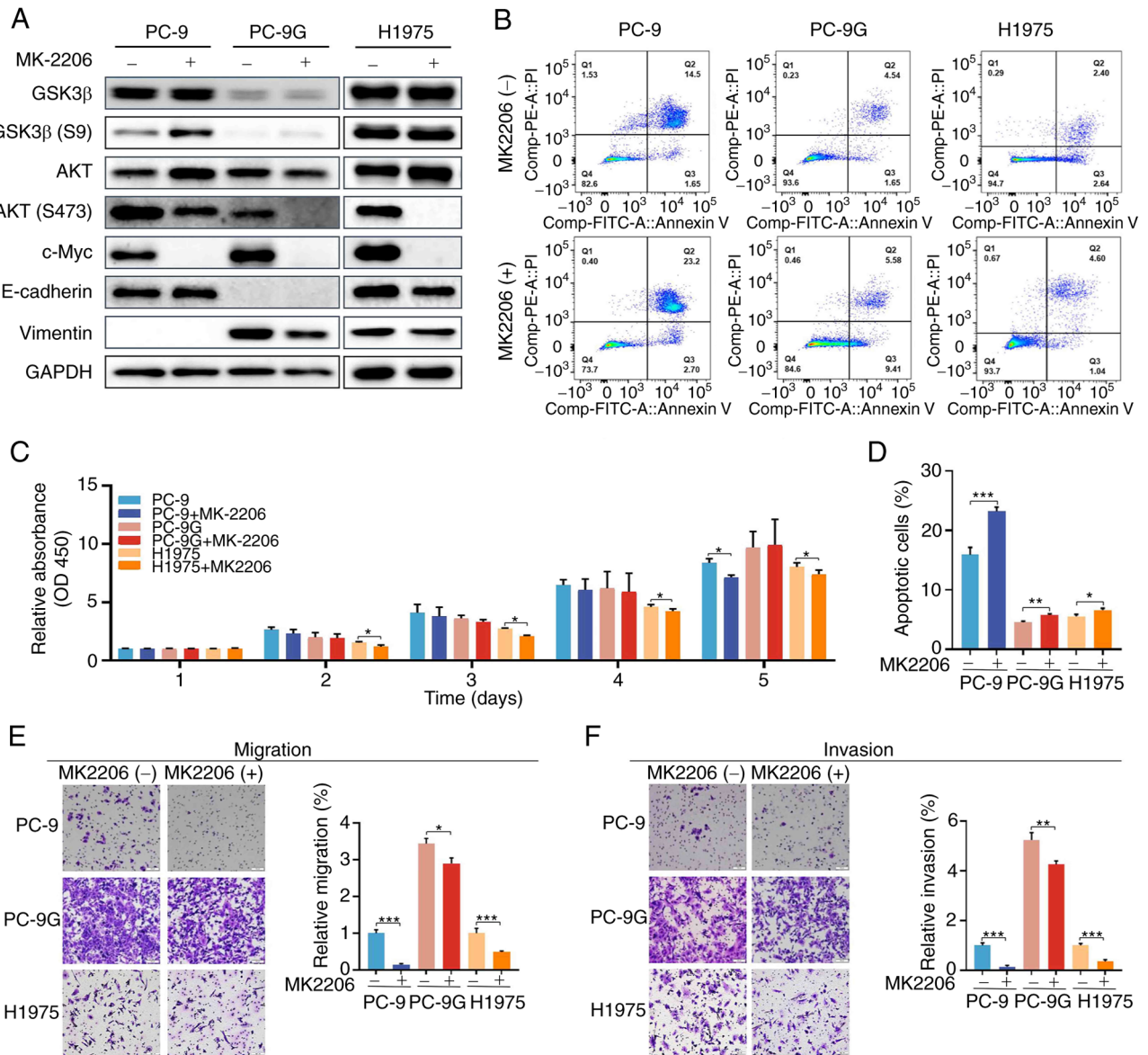
Figure 4. Effects of an AKT inhibitor on the proliferation, apoptosis, migration and invasion of PC-9, PC-9G and H1975 cells. (A) Protein expression levels of GSK3β, pGSK3β (Ser9), AKT, pAKT (Ser473), c-Myc, E-cadherin and vimentin were determined via western blot analysis in PC-9, PC-9G and H1975 cells treated with DMSO or 5 nmol/l MK2206. (B) Apoptotic rate of PC-9, PC-9G and H1975 cells was increased after MK2206 treatment. (C) MK2206 treatment inhibited the proliferation of H1975 cells from day 2 to 5 and reduced the proliferation of PC9 cells at day 5. (D) Quantification of apoptosis results. MK2206 treatment inhibited the (E) migration and (F) invasion of PC-9, PC-9G and H1975 cells (magnification, x20). Data are presented as the mean ± SD of three independent experiments. *P<0.05, **P<0.01, ***P<0.001. FITC, fluorescein isothiocyanate; GSK3β, glycogen synthase kinase 3β; p, phosphorylated; PC-9G, gefitinib-resistant PC-9; PI, propidium iodide.

without EGFR mutations, suggesting that the role of GSK3β may vary according to whether EGFR is mutated or not in gefitinib-resistant NSCLC.

The PI3K/AKT pathway serves a key role in cancer cells that are resistant to EGFR-TKIs (22,32), and AKT phosphorylates GSK3β at serine 9 (33,34). In the present study, AKT inhibition induced the apoptosis, and decreased the migration and invasion of PC-9, PC-9G and H1975 cells. By contrast, AKT activation increased the migration and invasion of PC-9, PC-9G and H1975 cells, and reduced the apoptosis of PC-9 cells. However, this pattern of AKT activation was inconsistent with that of GSK3β in PC-9G cells; thus, the activation of GSK3β may not be related to the AKT signaling pathway.

The Wnt/β-catenin pathway has a promotive effect on NSCLC cell proliferation and metastasis, leading to an increase in EGFR-TKI resistance in erlotinib-resistant NSCLC HCC827 cells (35,36). In the present study, cytoplasmic β-catenin and E-cadherin expression levels were reduced by overexpression of GSK3β in both PC-9 and H1975 cells. These findings are consistent with those of a previous study that reported that activation of the Wnt/β-catenin pathway leads to a decrease in cytoplasmic β-catenin expression (37), thereby promoting EMT and metastasis of NSCLC cells (30,38). A recent study demonstrated that GSK3β promotes gefitinib resistance by activating Wnt/β-catenin in PC-9 cells (39). However, in the present study, β-catenin expression was decreased in PC-9G cells compared with that in PC-9 cells, and GSK3β overexpression
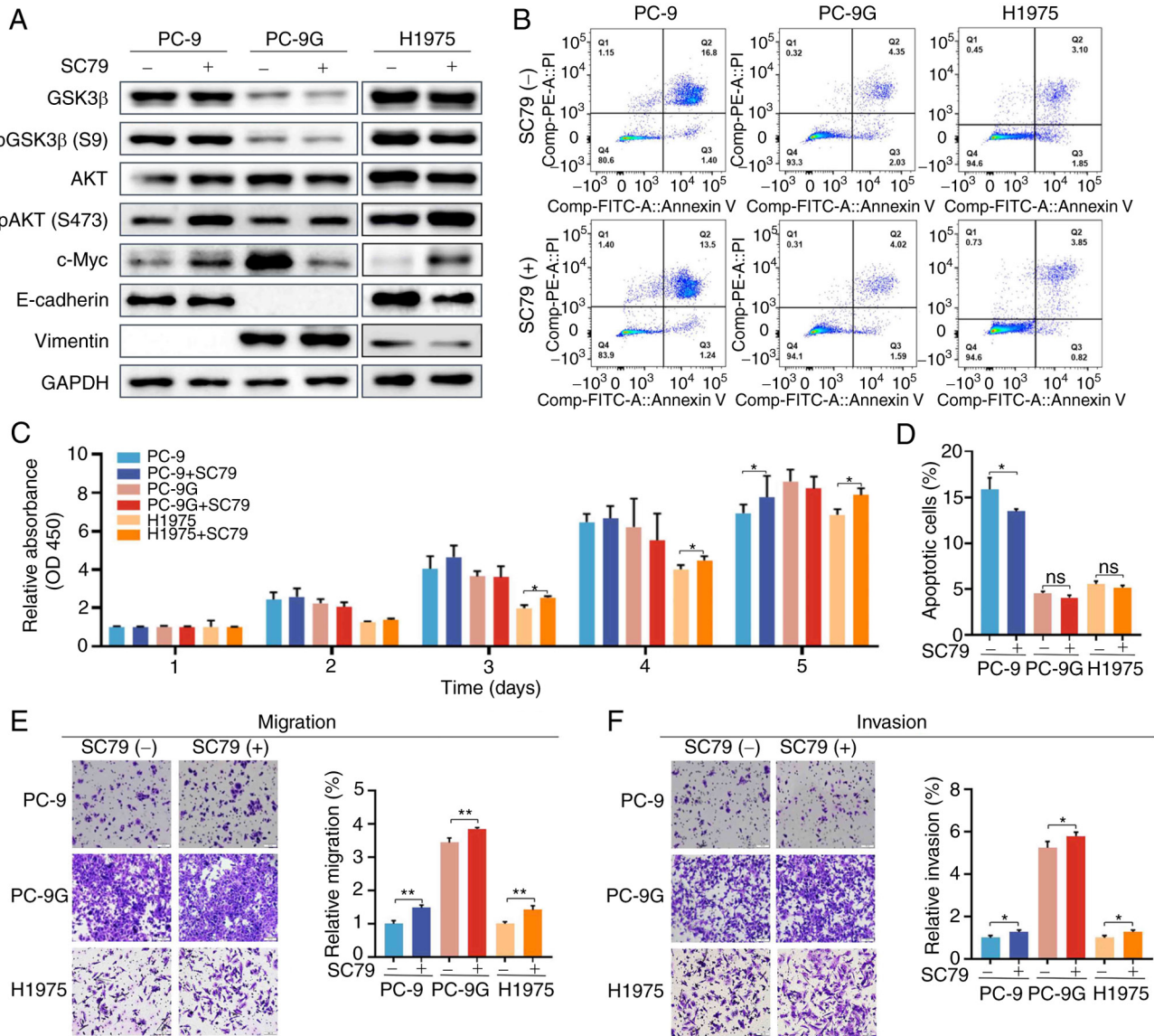
Figure 5. Effects of an AKT activator on the proliferation, apoptosis, migration and invasion of PC-9, PC-9G and H1975 cells. (A) Protein expression levels of GSK3β, pGSK3β (Ser9), AKT, pAKT (Ser473), c-Myc, E-cadherin and vimentin was determined via western blot analysis in PC-9, PC-9G and H1975 cells treated with DMSO or 5 nmol/l SC79. (B) Apoptotic rate of PC-9 cells was decreased after SC79 treatment. (C) SC79 treatment promoted the proliferation of PC-9 and H1975 cells. (D) Quantification of apoptosis results. SC79 treatment promoted the (E) migration and (F) invasion of PC-9, PC-9G and H1975 cells (magnification, x20). Data are presented as the mean ± SD of three independent experiments. *P<0.05, **P<0.01. FITC, fluorescein isothiocyanate; GSK3β, glycogen synthase kinase 3β; p, phosphorylated; PC-9G, gefitinib-resistant PC-9; PI, propidium iodide.

was insufficient to attenuate the already decreased cytoplasmic or nuclear β-catenin expression in PC-9G cells. It is difficult to determine whether GSK3β acts through the Wnt/β-catenin pathway in EGFR-resistant lung cancer without EGFR mutations, thus further studies are required.

In the present study, overexpression of GSK3β increased the proliferation, migration and invasion of PC-9 and H1975 cells. It has previously been reported that a GSK3 antagonist (CHIR99021), which inhibits both GSK3α and GSK3β, can inhibit the proliferation of human H1975 and H1299 NSCLC cell lines (40). However, knockdown of GSK3β, but not GSK3α, has been shown to induce a decrease in the proliferation of osimertinib-resistant H1975 cells (20), thus indicating that the functions of GSK3 isoforms are different. These findings indicated that GSK-3 isoforms exhibit important cell type-specific functions, which require further clarification.

A limitation of the present study is that it did not access the function of GSK3β in a gefitinib-resistant PC-9G xenograft model for *in vivo* functional validation. *In vivo* experiments are necessary steps for investigating the potential of a therapeutic strategy prior to clinical trials. In future, *in vivo* experiments should be performed to explore the suppressive role of GSK3β in gefitinib-resistant NSCLC.

In conclusion, the present study demonstrated that overexpression of GSK3β increased the proliferation, migration and invasion of gefitinib-resistant H1975 cells harboring the T790M and L858R mutations. Conversely, GSK3β overexpression reduced the proliferation, migration and invasion of PC-9G cells without EGFR mutations, suggesting that GSK3β serves a dynamic tumor-promoting or tumor-suppressive role in gefitinib-resistant lung adenocarcinoma cells depending on the type of EGFR mutation. Additionally, AKT inhibition

induced the apoptosis, and reduced the migration and invasion of PC-9, PC-9G and H1975 cells, and these effects were reversed following AKT activation; the function of GSK3β was not dependent on the tumor promotor role of the AKT pathway in PC-9G cells without EGFR mutations. Notably, the molecular mechanisms underlying the diverse effects of GSK3β among different EGFR mutation types in NSCLC remain to be elucidated, and the properties of GSK3β need to be carefully evaluated when developing a therapeutic strategy for EGFR-mutant NSCLC that targets GSK3β.

Acknowledgements

Availability of data and materials

The RNA-seq data are available in the Figshare repository (https://doi.org/10.6084/m9.figshare.23575992). The other datasets used and/or analyzed during the current study are available from the corresponding author on reasonable request.

Author's contributions

JL, SX and XX conceptualized and designed the study. XW and XJ acquired the data and drafted the manuscript. XJ and CH performed data analysis. JL, XW, XJ, SX and XX wrote the manuscript. SX and XX revised the manuscript. JL, SX and XX confirm the authenticity of all the raw data. All authors read and approved the final manuscript.

Ethics approval and consent to participate

Not applicable.

Patient consent for publication

Not applicable.

Competing interests

The authors declare that they have no competing interests.

References

1. Osmani L, Askin F, Gabrielson E and Li QK: Current WHO guidelines and the critical role of immunohistochemical markers in the subclassification of non-small cell lung carcinoma (NSCLC): Moving from targeted therapy to immunotherapy. Semin Cancer Biol 52: 103-109, 2018.
2. Lynch TJ, Bell DW, Sordella R, Gurubhagavatula S, Okimoto RA, Brannigan BW, Harris PL, Haserlat SM, Supko JG, Haluska FG, *et al*: Activating mutations in the epidermal growth factor receptor underlying responsiveness of non-small-cell lung cancer to gefitinib. N Engl J Med 350: 2129-2139, 2004.

3. Paez JG, Jänne PA, Lee JC, Tracy S, Greulich H, Gabriel S, Herman P, Kaye FJ, Lindeman N, Boggon TJ, *et al*: EGFR mutations in lung cancer: Correlation with clinical response to gefitinib therapy. Science 304: 1497-1500, 2004.
4. Zhou C, Wu YL, Chen G, Feng J, Liu XQ, Wang C, Zhang S, Wang J, Zhou S, Ren S, *et al*: Erlotinib versus chemotherapy as first-line treatment for patients with advanced EGFR mutation-positive non-small-cell lung cancer (OPTIMAL, CTONG-0802): A multicentre, open-label, randomised, phase 3 study. Lancet Oncol 12: 735-742, 2011.
5. Mitsudomi T, Morita S, Yatabe Y, Negoro S, Okamoto I, Tsurutani J, Seto T, Satouchi M, Tada H, Hirashima T, *et al*: Gefitinib versus cisplatin plus docetaxel in patients with non-small-cell lung cancer harbouring mutations of the epidermal growth factor receptor (WJTOG3405): An open label, randomised phase 3 trial. Lancet Oncol 11: 121-128, 2010.
6. Riely GJ, Politi KA, Miller VA and Pao W: Update on epidermal growth factor receptor mutations in non-small cell lung cancer. Clin Cancer Res 12: 7232-7241, 2006.
7. Kobayashi S, Boggon TJ, Dayaram T, Jänne PA, Kocher O, Meyerson M, Johnson BE, Eck MJ, Tenen DG and Halmos B: EGFR mutation and resistance of non-small-cell lung cancer to gefitinib. N Engl J Med 352: 786-792, 2005.
8. Pao W, Miller VA, Politi KA, Riely GJ, Somwar R, Zakowski MF, Kris MG and Varmus H: Acquired resistance of lung adeno-carcinomas to gefitinib or erlotinib is associated with a second mutation in the EGFR kinase domain. PLoS Med 2: e73, 2005.
9. Adams E, Sepich-Poore GD, Miller-Montgomery S and Knight R: Using all our genomes: Blood-based liquid biopsies for the early detection of cancer. View (Beijing) 3: 20200118, 2022.
10. Engelman JA, Zejnullahu K, Mitsudomi T, Song Y, Hyland C, Park JO, Lindeman N, Gale CM, Zhao X, Christensen J, *et al*: MET amplification leads to gefitinib resistance in lung cancer by activating ERBB3 signaling. Science 316: 1039-1043, 2007.
11. Thomson S, Petti F, Sujka-Kwok I, Epstein D and Haley JD: Kinase switching in mesenchymal-like non-small cell lung cancer lines contributes to EGFR inhibitor resistance through pathway redundancy. Clin Exp Metastasis 25: 843-854, 2008.
12. Sequist LV, Waltman BA, Dias-Santagata D, Digumarthy S, Turke AB, Fidias P, Bergethon K, Shaw AT, Gettinger S, Cosper AK, *et al*: Genotypic and histological evolution of lung cancers acquiring resistance to EGFR inhibitors. Sci Transl Med 3: 75ra26, 2011.
13. Yano S, Wang W, Li Q, Matsumoto K, Sakurama H, Nakamura T, Ogino H, Kakiuchi S, Hanibuchi M, Nishioka Y, *et al*: Hepatocyte growth factor induces gefitinib resistance of lung adenocarcinoma with epidermal growth factor receptor-activating mutations. Cancer Res 68: 9479-9487, 2008.
14. Oxnard GR, Arcila ME, Chmielecki J, Ladanyi M, Miller VA and Pao W: New strategies in overcoming acquired resistance to epidermal growth factor receptor tyrosine kinase inhibitors in lung cancer. Clin Cancer Res 17: 5530-5537, 2011.
15. Zheng X, Huang D, Liu X, Liu QY, Gao X and Liu L: GSK3β/ITCH/c-FLIP axis counteracts TRAIL-induced apoptosis in human lung adenocarcinoma cells. Protein Pept Lett 30: 242-249, 2023.
16. He L, Endress J, Cho S, Li Z, Zheng Y, Asara JM and Blenis J: Suppression of nuclear GSK3 signaling promotes serine/one-carbon metabolism and confers metabolic vulnerability in lung cancer cells. Sci Adv 8: eabm8786, 2022.
17. Alves M, Borges DP, Kimberly A, Neto FM, Oliveira AC, de Sousa JC, Nogueira CD, Carneiro BA and Tavora F: Glycogen synthase kinase-3 beta expression correlates with worse overall survival in non-small cell lung cancer-A clinicopathological series. Front Oncol 11: 621050, 2021.
18. Zeng J, Liu D, Qiu Z, Huang Y, Chen B, Wang L, Xu H, Huang N, Liu L and Li W: GSK3β overexpression indicates poor prognosis and its inhibition reduces cell proliferation and survival of non-small cell lung cancer cells. PLoS One 9: e91231, 2014.
19. Vincent EE, Elder DJ, O'Flaherty L, Pardo OE, Dzien P, Phillips L, Morgan C, Pawade J, May MT, Sohail M, *et al*: Glycogen synthase kinase 3 protein kinase activity is frequently elevated in human non-small cell lung carcinoma and supports tumour cell proliferation. PLoS One 9: e114725, 2014.
20. Fukuda K, Takeuchi S, Arai S, Kita K, Tanimoto A, Nishiyama A and Yano S: Glycogen synthase kinase-3 inhibition overcomes epithelial-mesenchymal transition-associated resistance to osimertinib in EGFR-mutant lung cancer. Cancer Sci 111: 2374-2384, 2020.
21. Nagini S, Sophia J and Mishra R: Glycogen synthase kinases: Moonlighting proteins with theranostic potential in cancer. Semin Cancer Biol 56: 25-36, 2019.

22. Nakata A and Gotoh N: Recent understanding of the molecular mechanisms for the efficacy and resistance of EGF receptor-specific tyrosine kinase inhibitors in non-small cell lung cancer. Expert Opin Ther Targets 16: 771-781, 2012.
23. Deng QF, Su BO, Zhao YM, Tang L, Zhang J and Zhou CC: Integrin β1-mediated acquired gefitinib resistance in non-small cell lung cancer cells occurs via the phosphoinositide 3-kinase-dependent pathway. Oncol Lett 11: 535-542, 2016.
24. Wang W, Xia X, Chen K, Chen M, Meng Y, Lv D and Yang H: Reduced PHLPP expression leads to EGFR-TKI resistance in lung cancer by activating PI3K-AKT and MAPK-ERK dual signaling. Front Oncol 11: 665045, 2021.
25. Wu SG and Shih JY: Management of acquired resistance to EGFR TKI-targeted therapy in advanced non-small cell lung cancer. Mol Cancer 17: 38, 2018.
26. Carlson M: org.Hs.eg.db: Genome wide annotation for human. 2019. R package version 3.10.0. https://bioconductor.org/packages/release/data/annotation/html/org.Hs.eg.db.html. 2020.
27. Livak KJ and Schmittgen TD: Analysis of relative gene expression data using real-time quantitative PCR and the 2(-Delta Delta C(T)) method. Methods 25: 402-408, 2001.
28. Schuhmacher M, Staege MS, Pajic A, Polack A, Weidle UH, Bornkamm GW, Eick D and Kohlhuber F: Control of cell growth by c-Myc in the absence of cell division. Curr Biol 9: 1255-1258, 1999.
29. Tsoukalas N, Aravantinou-Fatorou E, Tolia M, Giaginis C, Galanopoulos M, Kiakou M, Kostakis ID, Dana E, Vamvakaris I, Korogiannos A, et al: Epithelial-mesenchymal transition in non small-cell lung cancer. Anticancer Res 37: 1773-1778, 2017.
30. Song YA, Ma T, Zhang XY, Cheng XS, Olajuyin AM, Sun ZF and Zhang XJ: Apatinib preferentially inhibits PC9 gefitinib-resistant cancer cells by inducing cell cycle arrest and inhibiting VEGFR signaling pathway. Cancer Cell Int 19: 117, 2019.
31. Zhu Y, He W, Gao X, Li B, Mei C, Xu R and Chen H: Resveratrol overcomes gefitinib resistance by increasing the intracellular gefitinib concentration and triggering apoptosis, autophagy and senescence in PC9/G NSCLC cells. Sci Rep 5: 17730, 2015.
32. Sordella R, Bell DW, Haber DA and Settleman J: Gefitinib-sensitizing EGFR mutations in lung cancer activate anti-apoptotic pathways. Science 305: 1163-1167, 2004.
33. Dajani R, Fraser E, Roe SM, Young N, Good V, Dale TC and Pearl LH: Crystal structure of glycogen synthase kinase 3 beta: Structural basis for phosphate-primed substrate specificity and autoinhibition. Cell 105: 721-732, 2001.
34. Jope RS and Johnson GV: The glamour and gloom of glycogen synthase kinase-3. Trends Biochem Sci 29: 95-102, 2004.
35. Feng S, Liu H, Du P, Dong X, Pang Q and Guo H: Long non-coding RNA AC122108.1 promotes lung adenocarcinoma brain metastasis and progression through the Wnt/β-catenin pathway by directly binding to aldolase A. Ann Transl Med 9: 1729, 2021.
36. Wang Q, Liao J, He Z, Su Y, Lin D, Xu L, Xu H and Lin J: LHX6 affects erlotinib resistance and migration of EGFR-mutant non-small-cell lung cancer HCC827 cells through suppressing Wnt/β-catenin signaling. Onco Targets Ther 13: 10983-10994, 2020.
37. Shang S, Hua F and Hu ZW: The regulation of β-catenin activity and function in cancer: Therapeutic opportunities. Oncotarget 8: 33972-33989, 2017.
38. Roy LD, Sahraei M, Subramani DB, Besmer D, Nath S, Tinder TL, Bajaj E, Shanmugam K, Lee YY, Hwang SI, et al: MUC1 enhances invasiveness of pancreatic cancer cells by inducing epithelial to mesenchymal transition. Oncogene 30: 1449-1459, 2011.
39. Huang JQ, Duan LX, Liu QY, Li HF, Hu AP, Song JW, Lin C, Huang B, Yao D, Peng B, et al: Serine-arginine protein kinase 1 (SRPK1) promotes EGFR-TKI resistance by enhancing GSK3β Ser9 autophosphorylation independent of its kinase activity in non-small-cell lung cancer. Oncogene 42: 1233-1246, 2023.
40. O'Flaherty L, Shnyder SD, Cooper PA, Cross SJ, Wakefield JG, Pardo OE, Seckl MJ and Tavaré JM: Tumor growth suppression using a combination of taxol-based therapy and GSK3 inhibition in non-small cell lung cancer. PLoS One 14: e0214610, 2019.